Journal of Hydraulic Structures
J. Hydraul. Struct., 2020; 6(2): 56 - 79
DOI: 10.22055/jhs.2020.34021.1140

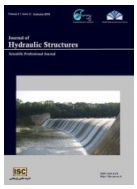

OPEN ACCESS

Near fault and far fault seismic analysis of concrete gravity dam

Prince Pundrik[1]
Ashish Bahuguna[1]
Mohd Firoj[2]

Abstract

Ground motions records of the past higher magnitude (M_w>5) earthquakes have indicated that ground motions recorded at the closest distance of the near-fault are very different from those recorded from a higher distance from the site of the far-fault. Forward directivity and fling effect are the essential characteristics of the near-fault earthquakes; these can cause potentially high damage during earthquakes. Hence, to understand the effect of the far-fault and near-fault on the performance of the structure is vital to reduce the damage and perform an efficient response. In this paper, an attempt is made to evaluate the effects of far-fault and near-fault ground motions on the seismic performance of the concrete gravity dam incorporating the dam-reservoir-foundation interaction. An arbitrary gravity dam is considered as numerical example. In this, eight different earthquake records are considered for time history analyses. The seismic performance of the dam is evaluated using the cumulative-overstress-duration (COD) and demand-capacity ratio (CDR). The results obtained show the importance of the near-fault ground motion effect on the seismic performance of the concrete gravity dam.

Keywords: Cumulative-overstress-duration, Dam, Demand-Capacity Ratio, Finite Element Analysis, Near Fault, and Far Fault.

Received: 17 June 2020; Accepted: 19 September 2020

[1] Earthquake Engineering Department, IIT Roorkee, Roorkee, Uttarakhand, India.
[2] Earthquake Engineering Department, IIT Roorkee, Roorkee, Uttarakhand, India, mohdfiroj2493@gmail.com, **(Corresponding Author)**

1. Introduction

In recent decades concrete gravity dams have been extensively constructed due to their simple structure, reliability, and safety and strong adaptability to geologic and topographic circumstances. Therefore, the seismic safety and seismic performance of the concrete gravity dam is a critical issue that must be addressed. Recent earthquake records such as Loma Prieta (1989), Kobe (1999), and Chi-Chi (1999) conceded that seismic strong ground motion records within the near-fault region are quite distinct from the general far-field ground motions recorded at a large distance in respect to various parameters such as PGA, PGV, PGD, rupture directivity, the period of the earthquake, pulse properties and fling step [1]. Fling effect and forward directivity have been as primary characteristics of near-fault ground motions [2]. Most studies relate the damaging potential of near-fault ground motions to velocity pulses. However, there are various opinions on this; [3] conclude that the damaging potential of near-fault depends on ground displacement occurs during velocity pulse. More thought should be directed towards the distinguishable acceleration pulse rather than the velocity pulse [4]. Various studies have been performed which have given significant insights on near-fault and far-fault ground motion. Story drift calculated based on near-fault ground motion s larger than that of far-fault motion [5-6]. The long pulse of near-fault motion is more critical for a long period structure than that of a short period structure [7]. The method, such as the square root of the sum of squares (SRSS) and the sum of absolute value (SAV), for estimating the inelastic displacement response of structure could give inconsistent results for near-fault ground motion [8]. Studies on the effect of near-fault and far-fault ground motion on seismic performance of dams [9-11] have considered the impact of far and near-fault ground motion and with non-linear dynamic response including dam-reservoir foundation interaction, and found that the non-linear response obtained from near-fault ground motions has a substantially different displacement response than that of far-fault ground motions. [12] investigate non-linear seismic response with near-fault and far-fault ground motion, including dam-water-sediment-foundation interaction. The elastoplastic behavior of the concrete dam is incorporated using the Drucker-Prager yield criterion. [13] investigated the structural response using elastic and inelastic response spectra far-fault and near-fault ground motion. They found that the strength and deformation demands of the fault-normal component of many near-fault ground motions are much higher than that of the fault-parallel part. Records suggest that a near-fault ground motion is characterized by a large high-energy pulse and a distinctive pulse shape for the velocity time history, median maximum demands, such as crest settlement and critical slip surface displacement of the embankment dam, were higher for near-fault ground motion than far-field motion[14]. Bayrakter et al., explored the impact of near field and far-fault ground movements on the seismic response of different kinds of dams [15], for example, concrete gravity dams, concrete faced rockfill, and clay-core rockfill dams. Wang et al., investigated the effect of the near field and far-fault ground movements on the seismic performance of concrete gravity dams [16]. Yazdani et al., found the proportional pulse in forward directivity (FD) and non-forward directivity (NFD) near field ground movements and examined the impact of pulse period on the response of concrete gravity dams [17]. The non-linear examination of dams demands more computational time than linear investigation. Ghanaat, proposed a standard and rational technique for performance assessment of concrete dams from linear time history investigation as stress Demand Capacity Ratio (DCR), Cumulative Inelastic Duration/Cumulative Overstress Duration (COD), and level of the overstressed area [18,19]. The Demand Capacity Ratio is characterized by Ghanaat, as "the proportion of the resulted principle stress to the tensile strength of concrete." The most extreme permitted DCR

for linear analysis of concrete dams is to relating for a pressure-demand double the tensile strength of concrete [18,19] . The total time of stress exceedance over a stress level related to a specific DCR is named as Cumulative Overstress Duration [16]. Recent earthquakes have shown the serious harm which occurred due to the fling step effect and forward directivity, both of which are essential attributes of near field ground movements [2]. Fig. 1 defines the three types of directivity effects that are neutral, reverse, and forward. If the hypocenter is normal to the Fault, neutral directivity happens. Longer duration and lower amplitude are attributes of reverse directivity, which is exhibited by rupture moving away from the site. When the site and Fault are lined up in the direction of the slip and movement of rupture front is towards the site, impacts of forward directivity can be seen. Strike-slip and dip-slip both have forward directivity impacts.

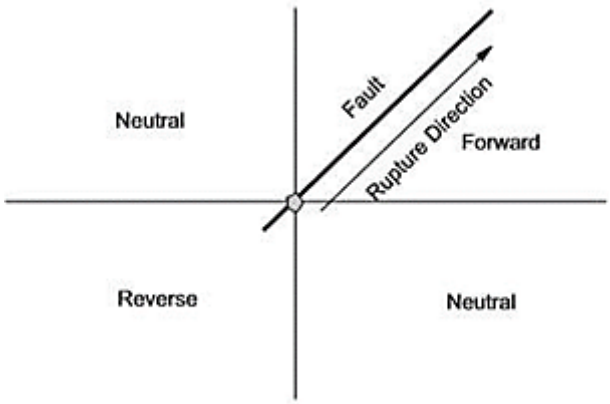

Figure 1.Defining the type of the directivity.

This paper deals with concrete dam response during considerably large earthquakes and forces on near-field and far-field effects in the full reservoir and rigid base conditions. The structures that are vibrating in the air and those surrounded by water are two different systems having different dynamics characteristics, and this is due to the interaction between structure and water, which results in hydrodynamic pressure and makes complications to the determination of dynamic forces. These oscillations result in impulsive and convective pressures. The convective pressures generally have insignificant magnitude, so convective pressures are neglected. The dam usually experiences the impulsive pressure as hydrodynamics pressures. From this fact, it can be said that the reservoir of the dam also interacts with the dam when it is subjected to dynamic loading due such as earthquakes. The magnitude and the distribution of stresses in different locations of the dam section can be determined for various static and dynamic loading conditions. The main objective of this analysis is to investigate the adequacy of the structure and the interaction of it with the foundation. The analysis is performed using a set of the ground motion recorded in both the near-field and far-field of recent earthquakes. Detailed, plausible damage that could occur in a dam due to both of the effects are presented using the linear time history analysis in terms of stress demand capacity ratio (DCR) and Cumulative Inelastic Duration/ Cumulative Overstress Duration (COD) analysis carried out with the help of FEM.

2. Characteristics of Near and Far Fault Earthquakes

There are various evident differences between earthquakes originating near to the Fault and far away from the Fault according to the recordings available [1]. The most prominent attributes

of near-fault ground movements are forward directivity and excursion impacts, as recognized by the researchers in this field [2]. Velocity pulses and large displacements are quite frequently observed in the normal segments of the Fault. Far-fault ground motions are not found with the articulated pulses that are characterized by the near field earthquakes. However, the attributes of near-fault ground movements, extensive damage, and colossal response are the possibilities of structure, which is resulting because of the high input energy at the start [20]. In far-fault earthquakes, the amplitude of the waves decreases with increasing site distance from the epicenter, which indicates that in far-fault effects, the amplitude should not be ignored. However, the duration time of the earthquake increased with an increase in epicenter distance, which leads to an increase in the period [21].

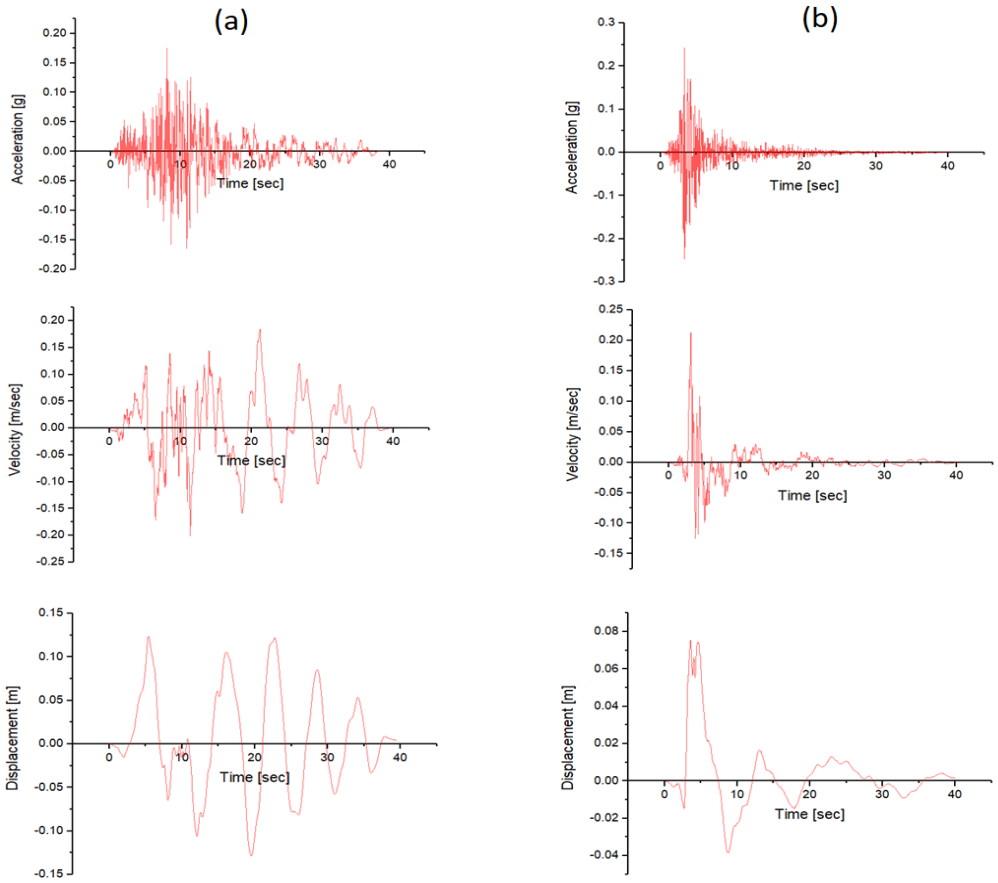

Figure 2.Time history example of acceleration, velocity, and displacement for (a) Far Field (b) Near Field of the Loma Prieta Earthquake.

The impacts of near-fault ground movements on numerous structural designing structures, for example, dams and towers, have been explored in numerous studies [16,22]. Recently done investigations and studies uncovered that there is an increasing demand for displacement and stresses when the dam is exposed to near-fault ground movements. Even though past examinations gave some data about the impacts of near-fault ground movements on the response of dams, concrete gravity dams are still not very well researched regarding the harm that can be caused due to the near-fault motions. Near field, ground movements are not just linked with

stable shaking but also with the geometry of Fault and direction in which the seismic wave is moving. The near field zone is commonly thought to be limited around a separation of 20 km [14] from the ruptured Fault; however, it is not universal and may be affected by several site conditions and ground motion. The fundamental recognized characteristics for the near field ground movements is the presence of unique, high-intensity large pulse (Fig. 2(b)) towards the start of the ground movement and which is evident at velocity time history [17].

3. Methodologies of Dam Modeling

The magnitude and the distribution of stresses in different locations of the dam section can be determined thoroughly for different static and dynamic loading conditions. Generally, approximate simplified methods or the finite element methods are used for the analyses of the dam depending upon the refinement needed. Concrete dams being brittle, most of the designs are based on conventional methods like allowable stress methods. However, in recent days the design philosophy of dams has changed concerned with the earthquake safety of dams. Gravity dams should be able to survive the Maximum Credible Earthquake (MCE) without any catastrophic failure resulting in loss of life and significant damage to property. MCE is the largest earthquake associated with a specific seismotectonic structure or source area within the regions of low seismicity. Linear analysis carried out with MCE results in tensile stresses exceeding greatly the tensile strength of the concrete calculated. Hence, the design philosophy is no longer valid since cracking is expected to occur in the dam sections. The problem worsens if the elastic dam is bonded perfectly to the foundation rock. The tensile stresses at the heel of the foundation under full reservoir conditions exceed the tensile strength of the concrete. With earthquake load acting on the dam system, the stresses will be still higher. To eliminate the undesirable stresses, the uneconomical remedial measures such as post-tensioning, dam thickening, and reinforcement would be necessary. Moreover, the engineers still adopting the conventional methods for design high tensile strength of mass concrete or small ground accelerations gives us no option but to come up with the performance criteria at both Design Basis Earthquake (DBE) and MCE levels. The equivalent static analysis, frequency (modal) analysis and linear dynamic method are few of the methodologies which are being used worldwide for analyses, stability, and performance of a concrete gravity dam.

3.1. Static analysis of gravity dam

Static analysis is the most simplified analysis of a structure where the effects of a sudden change in the structure are calculated without any long-term response due to that change on the structure. In the case of static analysis, the forces used in the dam sections are (1) Self-weight of the dam, (2) Hydrostatic forces due to the reservoir acting on the upstream face of the dam, (3) Uplift force acting at the base of the dam, (4) Silt load acting on the upstream side of the dam section, (5) Weight of water acting on the foundation in upstream. The force profiles hydrodynamic force acting on the dam section are shown in Fig. 3. For the static analysis, inertia and hydrodynamic loads are not considered. The boundary conditions are taken as fixed at the foundation base and as a roller on the foundation sides.

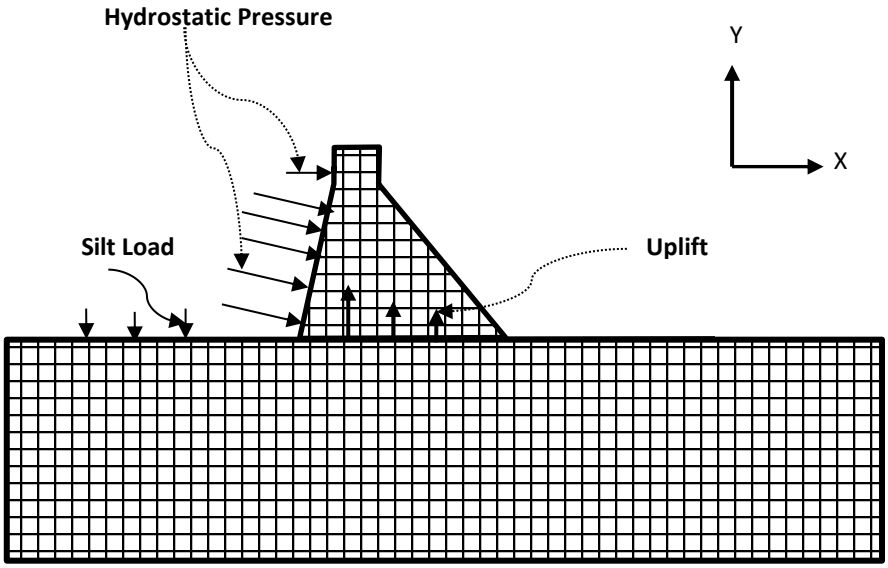

Figure 3.Static Loading in dam model

3.2. Frequency analysis (modal analysis)

Free vibration analysis of the dam is performed. Lancoz solver is used to determining the frequency of the dam section for different modes. This method is useful to find the mode shapes with their natural frequencies. The response of each mode can be calculated separately from this analysis. Mode superposition is carried out using the responses of different modes obtained from this analysis. Another critical parameter, mass participation factors of different modes, can be calculated using this method of analysis, which can tell us whether the multimode analysis is needed or not over the single-mode analysis.

3.3. Time History analysis

Time history analysis is a step-by-step analysis of the dynamic response of a structure to a specified loading (earthquake) that varies with time. Time history analysis is used to obtain a more accurate seismic response of the structure under the dynamic loading of a representative earthquake. In this type of analysis, the response of the structure at each time step specified can be obtained, which aids in properly studying the behavior of the structure. Another advantage of time history analysis is the ground motions/loading can be applied in multiple directions simultaneously.

Linear time history analysis is performed to get an idea of the behavior of the structure when subjected to the earthquake. The performance of the building in the linear range can be compared to the results obtained from other linear analyses like that of equivalent static analysis. Although linear time history analysis does not include the non-linear behavior of the structure, it could provide some insight into our study regarding the near field and far-field earthquakes.

In this paper, the model of the dam is subjected to accelerations from earthquake records that represent the expected earthquake at the base of the foundation. The dam section given in the problem is analyzed for Lumped mass with elementary boundary condition, and the deconvoluted time history is applied at the bottom of the soil or rock foundation. Dynamic assessment of gravity dams involves a vital part, selection of ground motion. In this

investigation, 16 earthquake records are chosen as the ground motions having both near field and far-field data. The selection of data has been carried out using the provisions of ASCE/SEI 7-16[23]. The ground motion selected are to be scaled either by amplitude scaling method or by spectral matching for a particular period range of the structure under consideration. This period range has an upper bound greater than or equal to 2 times the largest first-mode period, and a lower bound equal to the period at which at least 90% mass participation is achieved. The ground motions selected are then deconvoluted and applied at the base of the foundation rock.

3.4. Added mass approach as per IS 1893:1984

According to IS 1893: 1984[24], " if the height of the vertical portion of the upstream face of the dam is equal to or greater than one-half the total height of the dam, analyze it as if vertical throughout. If the height of the vertical portion of the upstream face of the dam is less than one-half the total height of the dam, use the pressure on the sloping line connecting the point of intersection of the upstream face of the dam and the reservoir surface with the point of intersection of the upstream face of the dam with the foundation". In the present dam geometry, the height of the vertical portion of the upstream face of the darn is less than the one-half height of the dam. Hence, it is not analyzed as vertical throughout for frequency extraction. Due to the horizontal acceleration of ground motion at the base of the dam, there is an instantaneous hydrodynamic pressure or suction exerted on the dam. Based on the assumption that the water is incompressible, the hydrodynamic pressure at depth 'y' below the reservoir surface shall be determined as follow.

$$P = C_s \alpha_h w h \tag{1}$$

Where, P = Hydrodynamic pressure in kg/m^2 at depth y, Cs= Coefficient, which varies with shape and depth, α_h= Design horizontal seismic coefficient, w = Unit weight of water in kg/ m^3, and h = Depth of reservoir in m. The variation of coefficient C_s with shapes and depths is illustrated in Appendix G of IS: 1893- 1984code[24]:

$$C_s = \frac{C_m}{2}\left\{\frac{y}{h}\left(2-\frac{y}{h}\right)+\sqrt{\frac{y}{h}\left(2-\frac{y}{h}\right)}\right\} \tag{2}$$

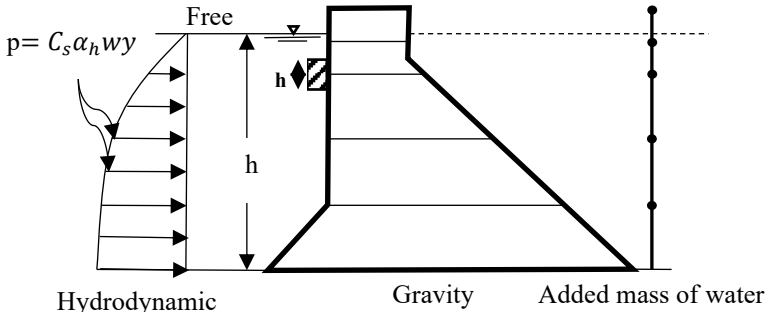

Figure 4. Hydrodynamic pressure distribution on the dam

Where, C_m = Maximum value of C_s, y = Depth below the water surface, h = Depth of the reservoir. The mathematical model consists of a lumped mass representation of the actual structure, as shown in Fig 4.

In the lumped mass system, the distributed mass of the structure is lumped at discrete points, and these masses are connected by massless elastic segments. As per IS Code, "for dams up to '100 in height, the seismic coefficient method shall be used for the design of the dams, while for dams over 100 m height, the response spectrum method shall be used. Both the seismic coefficient method (for dams up to 100 m height) and response spectrum method (for dams greater than 100 m height) are meant only for the preliminary design of dams"[25,26]. The design value of the horizontal seismic coefficient is calculated using the following expression given in IS 1893:1984 [24].

$$\alpha_h = \beta I F_o \frac{S_a}{g} \tag{3}$$

β = a seismic coefficient depending upon the soil-foundation, system I= Importance Factor (for the dam, I=3), F_o = seismic zone factor (avg. acceleration spectra), S_a/g = average spectral coefficient for appropriate natural period and damping of structure The fundamental period of vibration as per IS 1893:1984 is given as [24]

$$T = 5{,}55 \frac{H^2}{B} \left(\frac{\gamma_m}{g E_m}\right)^{0,5} \tag{4}$$

Where H = height of the dam in m, B = base width of the dam in m, γ_m= unit weight of the material of dam in N/m^3, g = acceleration due to gravity in m/s^2, and E_m = modulus of elasticity of the material in N/m^2.

3.5. Lumped Hydrodynamic Pressure

In the case of seismic analysis, the dynamic effect of the reservoir is undertaken by adding mass on the upstream face of the dam using the IS code approach. The height of the vertical portion of the upstream face of the dam is less than the one-half height of the dam. Hence, it is analyzed using the lumped pressure on the sloping line connecting the point of intersection of the upstream face of the dam and the reservoir surface. There are enough lumped masses in the model in order to represent the dominant frequencies of the gravity dam. Hence the value of C_m, in accordance to the slope, which is the maximum value of pressure coefficient for the sloping faces used for calculation of C_s, which is coefficient varying with shape and depth, is taken as 0.65 from IS 1893- 1984 [24]. Water is assumed to be incompressible. Inertial mass is added at the upstream side of the model in accordance to IS 1893-1984 [24] (Fig. 5).

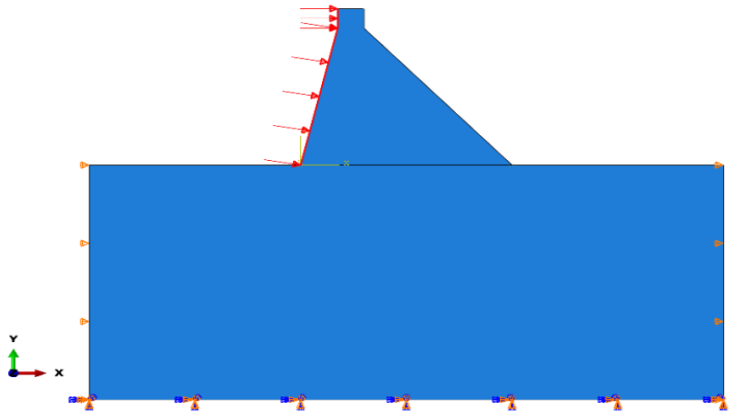

Figure 5.Lumped mass Hydrodynamic Pressure at the upstream of the Dam section.

4. Method to Evaluate the Seismic Performance

The seismic performance and assessment of the concrete gravity dam is estimated using DCR and the cumulative duration of the stress exceeding the tensile strength of the concrete and the overstressed regions. Demand-Capacity-Ratio, it is defined as the ratio of the maximum principal stress to (static) tensile strength of the concrete. Tensile strength characterized by the uni-axially splitting tensile test, or can be represented by the equation proposed by [27].

$$S_t = 1.7 S_c^{\frac{2}{3}} \tag{5}$$

Where, S_c is the compressive strength of the concrete, the maximum DCR for the linear analysis of dams is 2, this is corresponding to a stress demand twice the static tensile strength of the concrete [27]. Cumulative inelastic duration of stress propagation is defined as the total stress propagation above a stress level associated with DCR ≥ 1. Higher cumulative duration yields higher damage possibility. For concrete gravity dams, [19], have given a lower cumulative duration of 0.3s due to load resistance is based on the cantilever mechanism only. There is three performance level given by [19], (1) Minor or no: dam response is considered as elastic if the DCR ≤ 1. (2) DCR >1, the dam shows the non-linear response in the form of joint opening and cracking; if DCR>2, the overstressed regions are limited to 15% of the dam cross-section area. (3) Severe damage: DCR >2 or the COD for all DCR values range from 1, and 2 falls above the performance curves.

Table 1a. Input data for far fault ground motion

S. No.	Earthquake	Year	Station	M_w	Distance (km)	Vs30 (m/sec)	PGA (m/sec^2)	PGV (m/sec)	PGV/PGA (sec)
1	Loma Prieta	1989	Hayward City Hall-North	6.93	55.11	735.44	2.215	0.16	0.072
2	Kobe	1995	MZH	6.90	70.26	609	2.288	0.152	0.066
3	Chi-Chi	1999	HWA002	7.62	56.93	789.18	1.902	0.166	0.087
4	Duzce	1999	Lamont 1060	7.14	25.88	782	2.256	0.176	0.078
5	Hector Mine	1999	Banning - Twin Pines Road	7.13	83.43	667.42	2.9009	0.191	0.066
6	Tottori	2000	SMNH11	6.61	40.08	670.73	2.138	0.137	0.064
7	Chuetsu-oki	2007	Tokamachi Chitosecho	6.80	30.65	640.14	2.265	0.168	0.074
8	Iwate	2008	Maekawa Miyagi awasaki City	6.90	74.82	640.14	2.744	0.129	0.047

Table 1b: Input data for near-fault ground motion

S.No.	Earthquake	Year	Station	M_w	Distance (km)	Vs30 (m/sec)	PGA (m/sec2)	PGV (m/sec)	PGV/PGA (sec)
1	Loma Prieta	1989	Gilroy - Gavilan Coll	6.93	9.96	729.65	2.42	0.251	0.104
2	Kobe	1995	Nishi-Akashi	6.9	7.08	609	2.084	0.286	0.137
3	Chi-Chi	1999	TCU071	7.62	5.8	624.85	1.598	0.261	0.163
4	Duzce	1999	Lamont 531	7.14	8.03	638.39	1.785	0.327	0.183
5	Hector Mine	1999	Hector	7.13	11.66	726	1.526	0.263	0.172
6	Tottori	2000	SMN015	6.61	9.12	616.55	2.237	0.256	0.114
7	Chuetsu-oki	2007	Kashiwazaki Nishiyamacho Ikeura	6.8	12.63	655.45	2.189	0.282	0.129
8	Iwate	2008	IWT010	6.9	16.27	825.83	1.9	0.228	0.12

4.1. Input ground motion records

The time history earthquake data helps us compute deformation, stresses more accurately by considering the time-dependent nature of the dynamic response to earthquake ground motion. The near-field and far-field earthquake data have been obtained from the PEER database [28] .A total of 16 earthquakes have been selected, 8 of them being near field, and the other 8 being far field. The near field data being selected is having an apparent velocity pulse with pulse duration being more than 1 sec. Also, in addition to that ratio of PGV/PGA was checked to be more than 0.1 seconds. The far-field data is selected from the same site conditions and the same earthquake with the epicenter being at a larger distance. The data selected has the magnitude of Mw > 6.5, shear wave velocity around 800 m/s, and fault distance is considered to be within 20 km for near-fault and more than 20 km for far fault earthquakes with consideration of the PGV/PGA ration higher than and less than 0.1 respectively (Table 1). The ground motions were selected on the base of their corresponding acceleration spectra with the target spectrum (IS Code 1893 design response Spectrum).

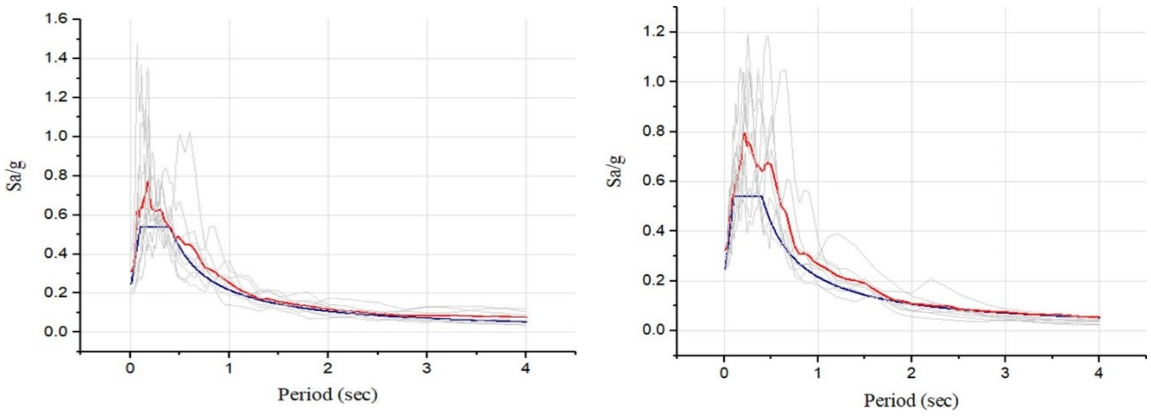

(a) (b)

Figure 6.(a) Far-fault average response spectrum (b) near-fault average response spectrum

The Amplitude scaling method, according to ASCE 7-16[23], recommends that the average of the acceleration spectrum of all the earthquakes should be higher than 0.9 times that of the target acceleration spectrum. The current target spectrum is the IS code spectrum for MCE (Maximum Credible Earthquake) for zone IV and soil type I given by IS 1893-2016 [29]. From Fig. 6, it is observed that the average of earthquakes considered is above 90 percent of the target acceleration spectrum.

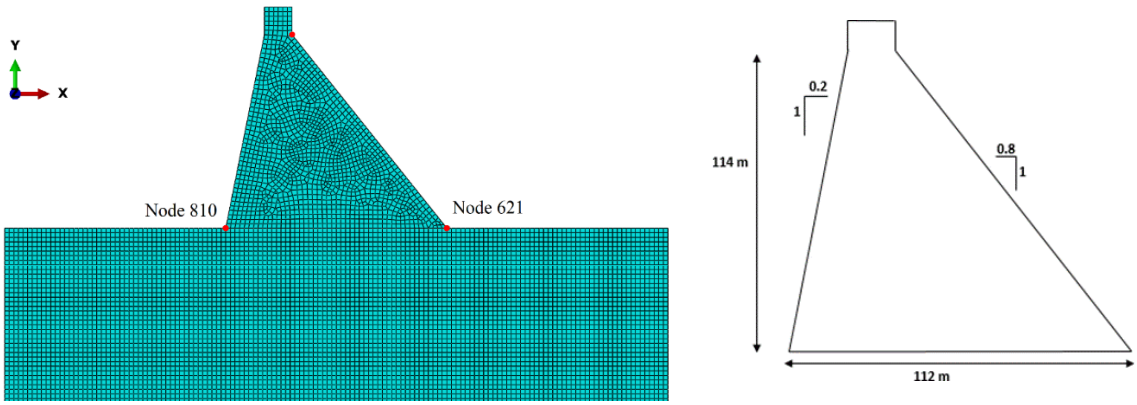

(a) (b)

Figure 7.(a) Finite element model of the Dam-Foundation System and (b) physical dimension of the dam model.

4.2. Finite Element model of Dam and Material Properties

The three-dimensional model of the concrete gravity dam reservoir system is assumed to be two dimensional after assuming that the geometry and properties of material do not change along the z-axis (Fig. 7(a)). Seismic analysis of buildings and other engineering structures is often based on the assumption that the foundation is rigid, which is subjected to unidirectional horizontal ground acceleration. The type of interaction between dam and foundation, as well as dam and reservoir, have a massive impact on the response achieved by the concrete gravity dam after subjecting to seismic ground motion. The simplified techniques generally neglect the interaction between the dam-reservoir-foundation systems, in contrast to the various rigorous

methods proposed by researchers range from finite element modeling to boundary integral equations. The gravity dam geometry considered for the present study is shown in Fig. 7(b). A 2-D FEM analysis of the dam foundation system has been carried out using the ABAQUS software package. A concrete gravity dam with a height of 114m, a base width of 112m, a downstream slope of 1:0.8, and an upstream slope of 1:0.2, is considered for numerical analysis. The material properties of the dam used in the analysis are shown in Table 2.

Table 2.Material properties of the dam

Material properties of the dam	Concrete	Foundation Rock	Reservoir
Elastic Modulus (*GPa*)	30	16.5	-
Poisson's Ratio (*v*)	0.2	0.33	-
Density (Kg/m^3)	2500	2600	1000
Bulk Modulus (GPa)	-	-	2.07

In the 2D model of the dam foundation system, CPE8R (8-node biquadratic, reduced integration) element is used to model both dam and foundation elements. ABAQUS 2D plane strain element CPE8R is shown in Fig. 8. This element is defined by eight nodes having two degrees of freedom at each node, translation in the nodal x, and y directions. As there are no particular design criteria for the fixing of mesh density, it is done by a trial and error method, optimizing the acceptable accuracy and computation time. A convergence study has been carried out to optimize the element size for the dam body and foundation. An element size of 2.5m for both Dam and Foundation has been finalized for the present finite element analysis of the concrete gravity dam.

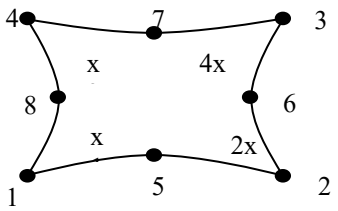

8-noded reduced

Figure 8.Geometry of CPE8R Element

Convergence analysis is carried out for different mesh sizes using time history analysis. Stress in a vertical direction (S22) at the heel has been considered for the study, and Loma Preita at near-fault is considered for time history loading (Table 1). Mesh sizes considered are 8m, 6m, 5m, 4m, 3m, 2.5m, and 2m, of which stress convergence is observed at a mesh size of 2.5m (Fig. 9). Considering both computation time and optimization of result, the mesh size of 2.5m is considered for analysis.

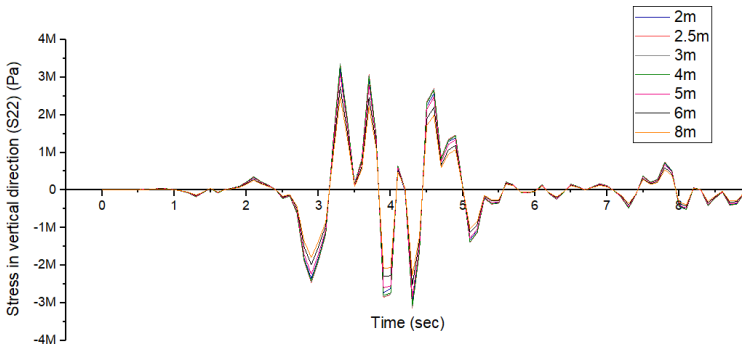

Figure 9. Stress plot for different mesh sizes

4.3. Dam-Reservoir-Foundation system

The foundation is considered to be a simplified massless body of 240 m in length along both the directions and 180 m in depth. The estimate of the foundation extent is calculated by convergence studies with varying sizes of the width of the foundation, which is necessary to produce accurate results that must be included in the FEM models to produce stresses in the dam. The foundation width of 2 times the width of the dam on each side and depth of 1.5 times the width of the dam is finalized for finite element modeling of foundation, and this is also supported by the manual by U.S. army corps. All the vertical grids are restrained from horizontal displacement, and all the horizontal grids are restrained from vertical displacement. The foundation is modeled using 2D plane strain elements. The earthquake motion is applied at the base of the rock opposite to the x-direction to meet the critical condition. The dam is resting on the rock foundation. The two sides of the foundation are supported by roller with movement allowed in the vertical direction in case of static analysis. In the case of dynamic analysis, the ground motion is applied at the base of the foundation.

4.4. Free Vibration Characteristics

A modal analysis is carried out in ABAQUS of the dam body to understand the free vibration characteristics and also the predominant frequencies of the structure. The first four typical mode frequency and shapes are shown in Table 3 and Fig. 10, respectively.

Table 3. Natural frequencies and natural time periods of the first four modes.

Mode	Frequency (Hz)	Time Period (sec)
1	2.094	0.47757
2	3.583	0.27911
3	4.074	0.24547
4	5.012	0.199525

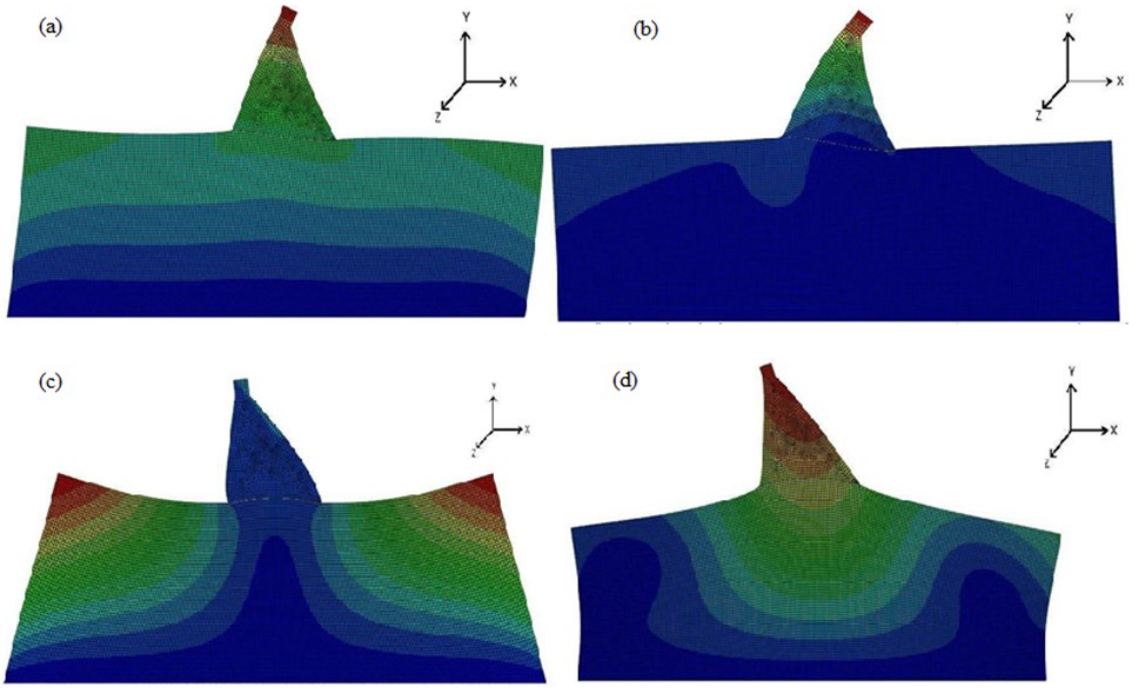

Figure 10.Showing the Mode shapes of the Dam System

4.5. Model Validation

The numerical model is validated with the analytical approach, and results are compared in terms of stress at the heel. The stress at the heel is calculated using the relation $(P_v)_{heel} = \frac{\sum V}{b}\{1 - \frac{6e}{b}\}$. Where, $(P_v)_{heel}$ is the stress at the heel, $\sum V$ = total vertical force, e = b/2 – X_c, and $X_c = M/\sum V$, M is the total moment about the toe. The total moment is calculated resisting moment minus the overturning moment. From Table 4, it can be noted that there is a good agreement with the results of the analytical approach and numerical approach using the ABAQUS.

Table 4. Stress calculated and Obtained from FEM model analysis at the heel of the Dam section.

	Heel	
Stress (MPa)	Analytical Approach	ABAQUS
	0.1384	0.1513

4.6. Ground Response Analysis

Ground Response Analysis (GRA) is carried out for further study related to reflecting waves from the truncated boundary. Loma Preita earthquake is considered for analysis (Table 1), and a 2D and 1D analysis is carried out using ABAQUS and DEEPSOIL v6.1, respectively. Deconvoluted earthquake is applied at the base of the foundation in the 2D FEM model considering the elementary boundary condition and response is calculated.

The same earthquake is then applied in the 1D model using DEEPSOIL v6.1, which is considered a boundary to be of infinite extent, and the response is calculated. The above two responses are then compared, shown in Fig. 11, and the result indicated that reflecting the wave is accounted for. Also, it has been observed that the response estimated from ABAQUS is a bit delayed than that of DEEPSOIL because the analysis was carried out in 2D and 1D, respectively.

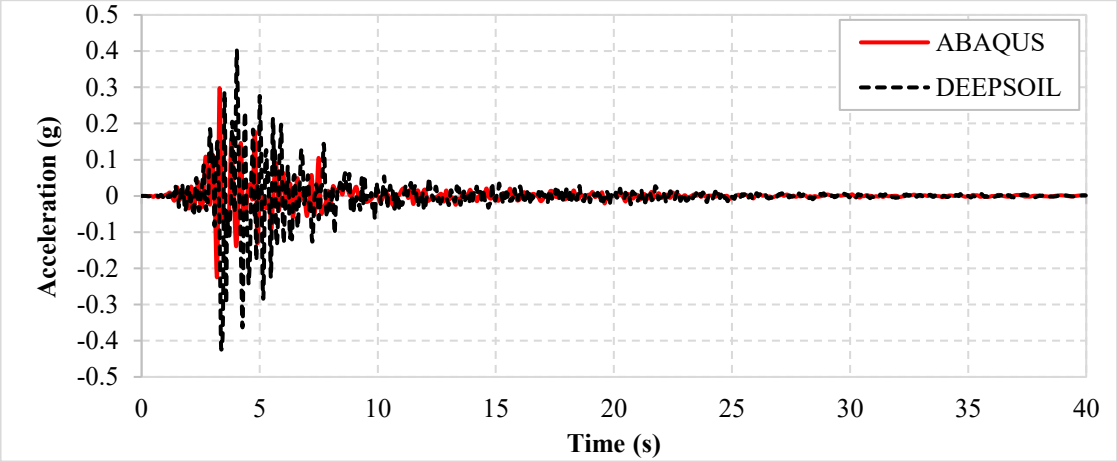

Figure 11.Comparing the response of ABAQUS and DEEPSOIL.

5. Result and Discussion

The force profile acting on the dam section is shown in (Fig. 3). Static analysis has been carried out on the dam reservoir foundation system considering static loads, gravity load, hydrostatic load, uplift press on the dam, and weight of water on the foundation alone. For static analysis, the boundary condition is taken as fixed at the foundation base and roller at the foundation sides. The maximum principal stresses developed are at the heel and toe of the dam, the maximum principal stresses presented in Table 5. Here positive principle stresses are taken as tension and negative principle stresses as compression, max principal stresses are shown in Fig. 12.

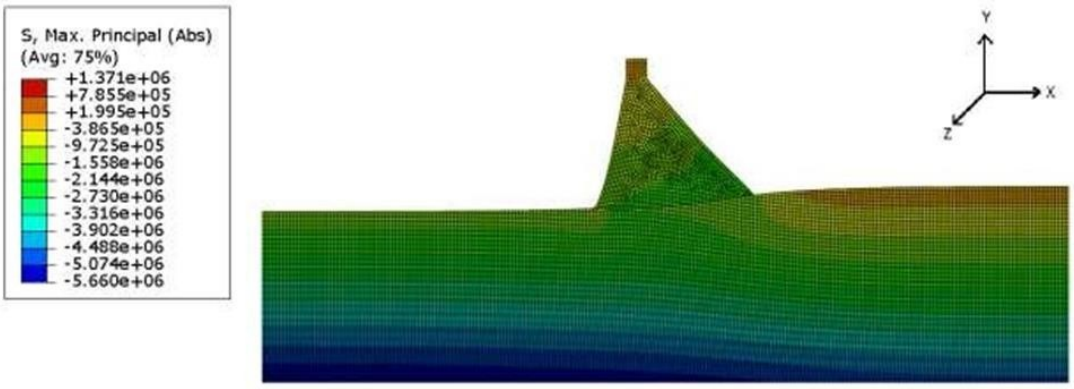

Figure 12.Principal stresses after initial static analysis

Table 5. Major Principal Stresses (MPa)

Toe (node 621)	Heel (node 810)
- 1.55	0.812

The values developed are well within the limiting static tensile strength of 3.0 MPa calculated as per Raphael, 1984 [27]. The time history results for stresses were analyzed for three nodes (Fig.7 a); however, after analyzing the maximum stresses for critical nodes, it is observed that cracking initiates and propagates at the toe and heel of the dam, so only these two nodes were considered for further comparative study. The plot of time history for stresses at these two nodes are shown (Fig. 13) for different earthquakes comparing both near field and far-field earthquakes. The results indicate that the stresses in the node 621(heel) and 810(toe) exceed the DCR = 1 and 2 values. DCR 1 corresponds to the tensile strength of 3 MPa, and DCR = 2 corresponds to the apparent dynamic tensile strength of 6 MPa [27]. The dam model is analyzed for the combined effect of static and seismic loads. Uplift pressure is assumed to be not changing during the application of seismic loading. Analysis results consist of principal stress, the time history of stresses comparing the near field, and far-field data in indication with Demand Capacity Ratio (DCR) limits. It can be observed from Fig. 13 that the exceedance of the stress cycle above DCR = 1 and DCR = 2 is more in a near-fault earthquake than far fault earthquake; also, stress obtained from the near-fault earthquake is more as compared to the far fault earthquake for both toe and heel. It could be due to a long period pulses in a near-field earthquake as they transmit large amounts of energy to the structures in a short time, and under such conditions, high energy dissipation demand increases. Which is likely to accumulate in the weakest parts of the dam [30]; however, the PGA is higher in the near-field as compared to the far-field earthquake for the corresponding period of the dam system (Fig 14), which also could be the reason for higher damage in the structure due to near field earthquake.

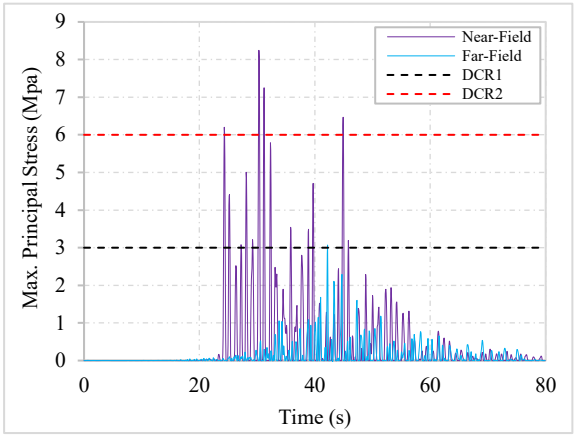

Chi-Chi at Node 621

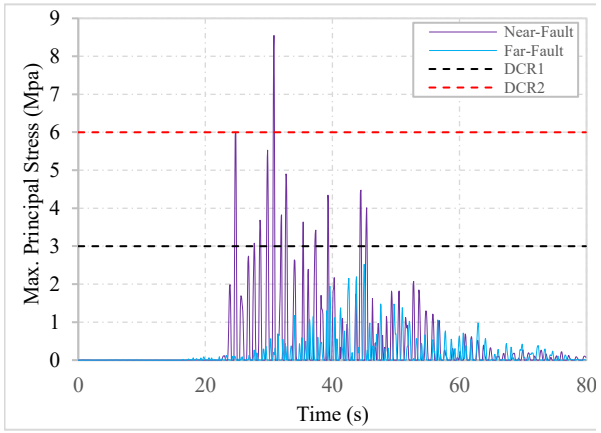

Chi-Chi at Node 810

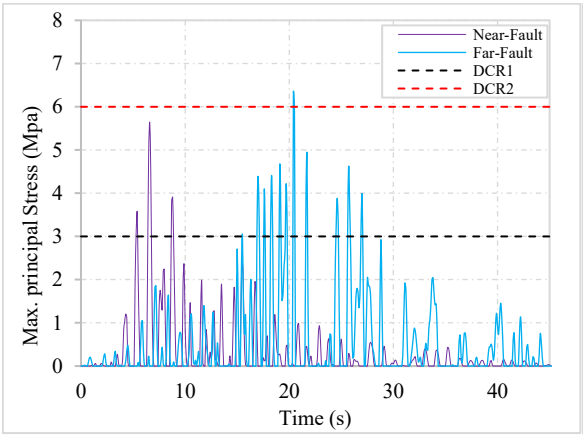

Hector-Mine at Node 621

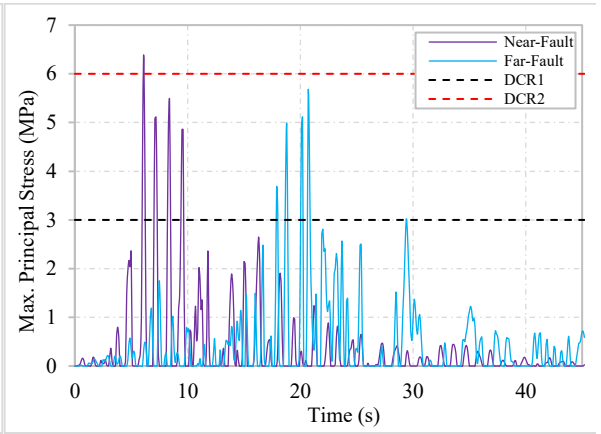

Hector-Mine at Node 810

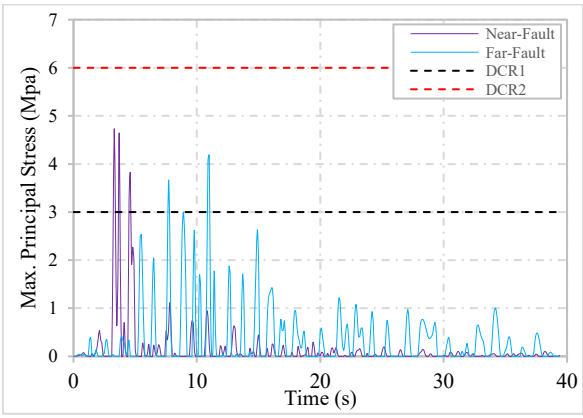

Loma Preita at Node 621

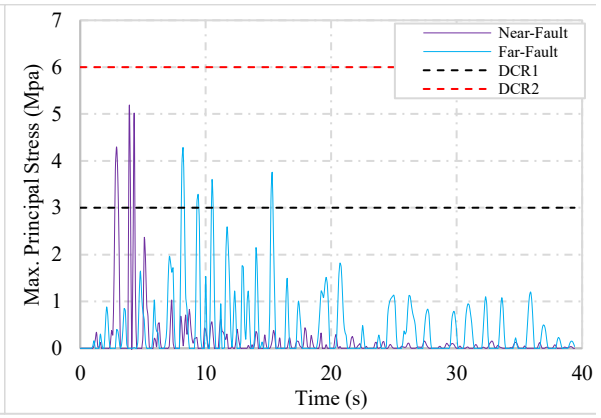

Loma Preita at Node 810

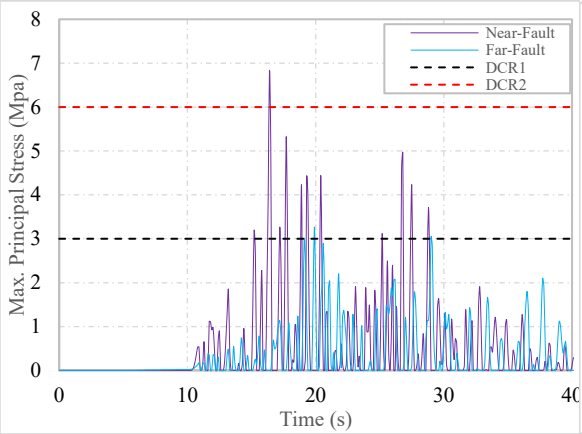

Duzce Turkey at Node 621

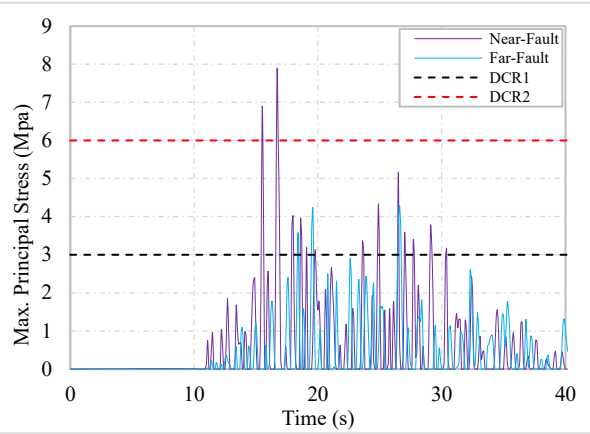

Duzce Turkey at Node 810

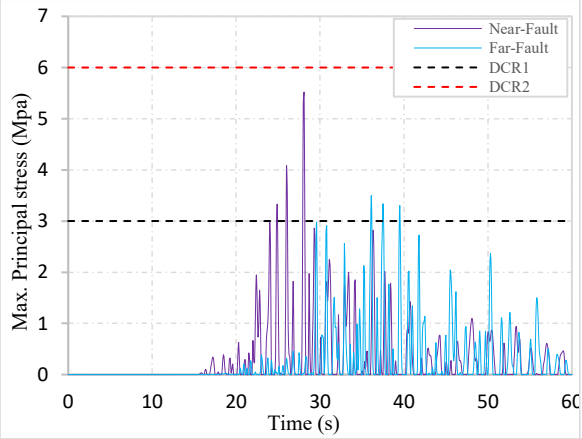

Iwate Japan at Node 621

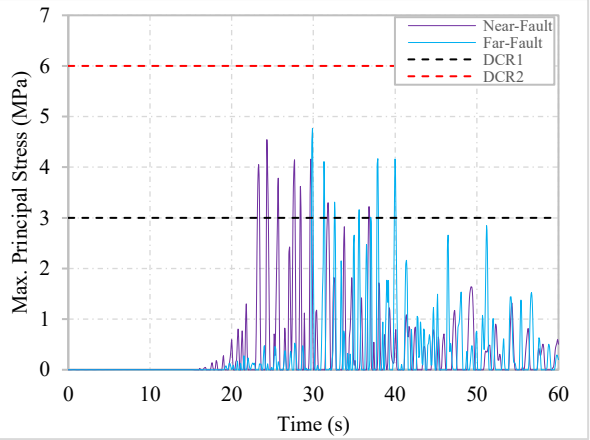

Iwate Japan at Node 810

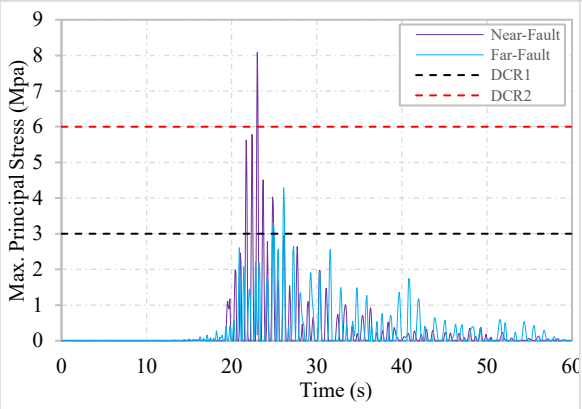

Chuefsu-obe Japan at Node 621

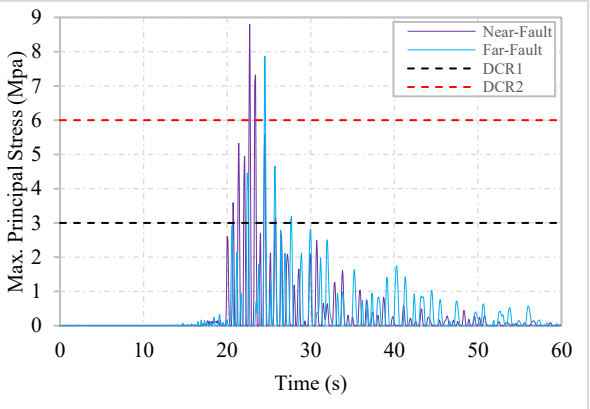

Chuefsu-obe Japan at Node 810

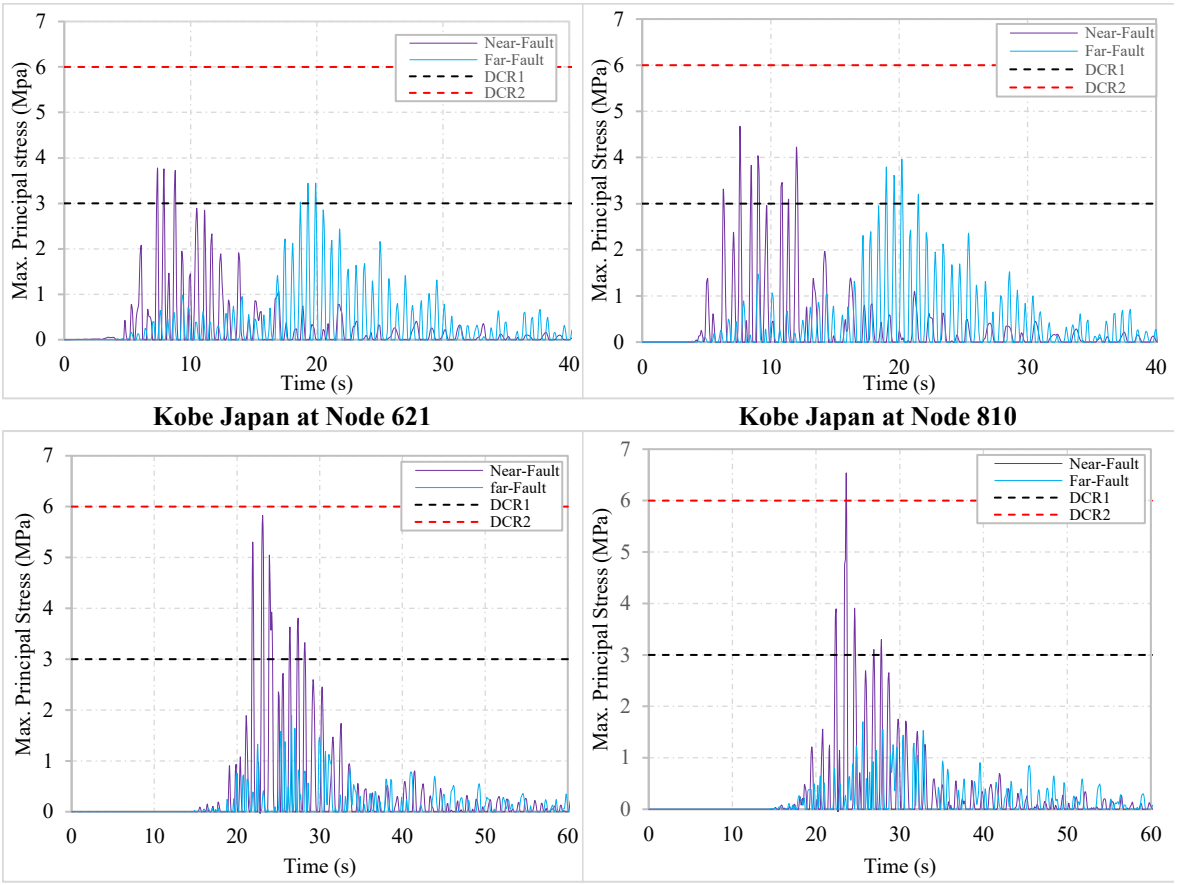

Figure 13.Maximum stress time history for the dam section

Further performance assessment has been analyzed using DCR vs. cumulative inelastic duration curve. Cumulative inelastic duration is the total time of stress exceedance in the time history of stresses above the particular DCR level. The comparison of the cumulative inelastic duration of nodes for different earthquakes is shown separately (Fig. 15). Fig. 15 depicts that the stresses at nodes 621 and 810 at heel and toe, respectively, are exceeding the acceptable limits of cumulative inelastic duration; this suggests that cracking may initiate at the heel and toe of the element and propagate through the body of the dam. The DCR values are going well beyond the limit for near-fault earthquakes for both toe and heel; also, it can be seen that far fault results are within the limit in some cases and might not cause failure to any node of the dam. Some tensile cracking may occur; however, there is no possibility of failure as the number of overstressing nodes are significantly less. Hector Mine and Loma Preita earthquakes at heel have a larger value for far-fault earthquakes near DCR=1; however, after analyzing principal stress results in ABAQUS, the area of overstress region was more in case of near-fault than far-fault.

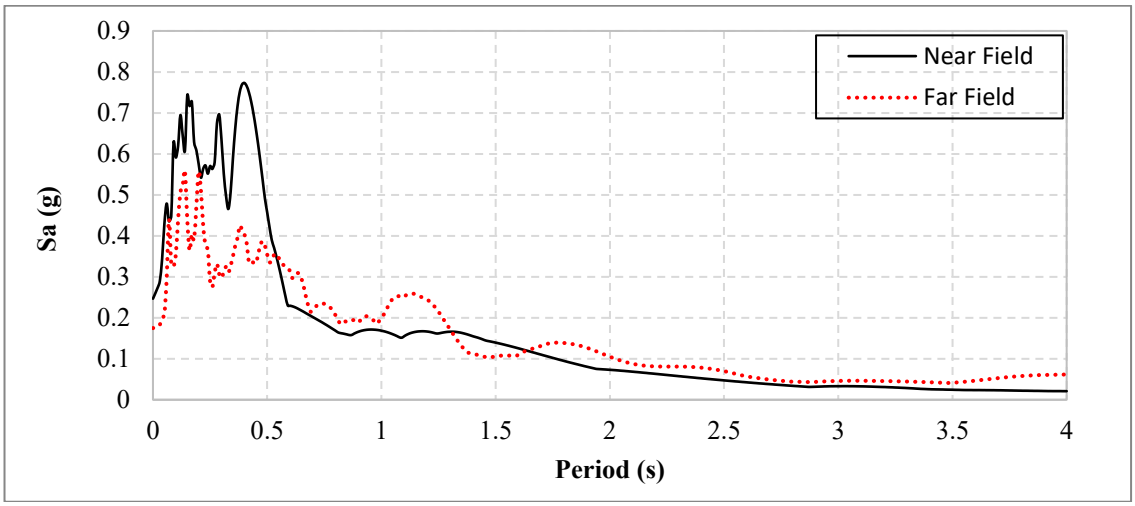

Figure 14.Showing the response spectrum of the near field and far-field of the Loma Prieta earthquake.

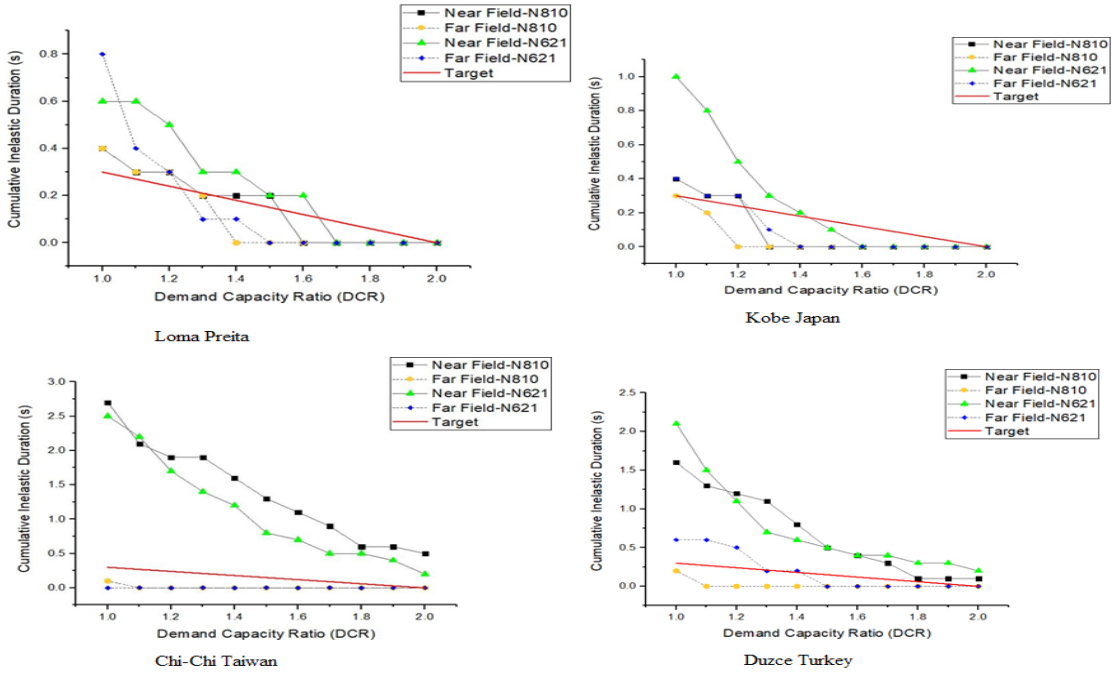

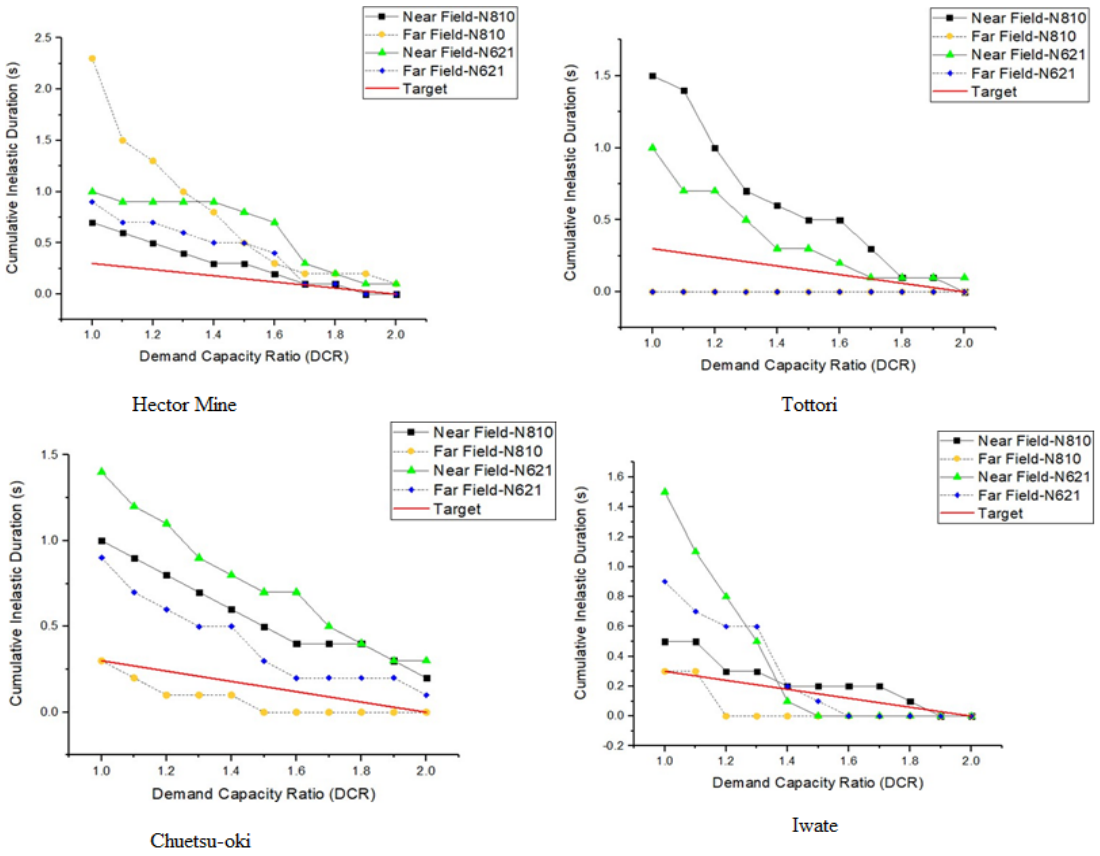

Figure 15.Performance assessment curve for the dam system

6. Conclusion

Series of linear analysis has been performed on the dam foundation system, and the time history of stresses are plotted. Modeling of the dam is carried out on ABAQUS software for plane strain conditions, and a total of 16 ground motions are applied as input excitation. DCR limits with cumulative inelastic duration for various critical elements in the dam are plotted, and the following are the conclusions.

- Linear elastic time history analysis is used to observe the dynamic behavior of the dam under near-fault and far fault ground motions.
- The results of the linear analysis are used to identify the potential failure modes of the dam.
- The results showed that the dam would experience cracking at the toe and heel portions of the dam. Comparing the effect of near and far fault earthquake on stress and cumulative inelastic duration curves, it can be concluded that near-fault is more effective and causes more damage than far fault earthquake and should be taken under consideration for more realistic results.

- According to the performed studies, as the near field records have pulses with long period (or shorter frequency), they have more impact on the dam in comparison to far field.
- Performance assessment shows that the seismic response of a concrete gravity dam is more under near-fault earthquake because of their severe and impulsive effect on structures.
- Since the post-earthquake stability of the dam is not carried out, a quantitative estimate of the stability of the dam for the post-earthquake condition is also necessary to ascertain and support the performance evaluated for the present system.
- The results showed that the dam would experience cracking at the toe and heel portions of the dam, and it required further non-linear analysis to understand the behavior of the concrete gravity dam**.**

Acknowledgment

The authors are thankful for the anonymous reviewer for their critical comments and suggestions, and the editor to improve the manuscript.

References

1. Chopra, A.K, Chintanapakdee C. (2001). Comparing response of SDF systems to near-fault and far-fault earthquake motions in the context of spectral regions. Earthq Eng Struct Dyn 30(12):1769–1789.
2. Mavroeidis, G.P., Papageorgiou A.S. (2003) A mathematical representation of near-fault ground motions. Bull Seismol Soc Am 93(3):1099–1131.
3. Hall, J.F., Heaton, T.H., Halling, M.W., Wald, D.J., (1995). Near-source ground motion and its effects on flexible buildings. Earthquake Spectra 11, 569–605.
4. Makris, N., Black, C., (2003). Dimensional analysis of inelastic structures subjected to near-fault ground motions. Report No. 03-05. California Earthquake Engineering Research Center, University of California, Berkeley, pp. 89–91.
5. Chopra, A.K., Chintanapakdee, C., (2001b). Drift spectrum versus modal analysis of structural response to near-fault ground motions. Earthquake Spectra 17 (2), 221–234.
6. Kalkan, E., Kunnath, S.K., (2006). Effects of fling-step and forward-rupture directivity on the seismic response of buildings. Earthquake Spectra 22 (2), 367–390.
7. Alavi, B., Krawinkler, H., (2004). Behaviour of moment resisting frame structures subjected to near-fault ground motions. Earthquake Engineering and Structural Dynamics 33, 687–706.
8. MacRae, G.A., Morrow, D.V., Roeder, C.W., (2001). Near-fault ground motion effects on simple structures. Journal of Structural Engineering 127 (9), 996–1004.
9. Ohmachi, T., Kojima, N., (2003). Near-field effect of hidden seismic faulting on a concrete dam. Natural Disaster Science 25, 7–15.
10. Hadiani, N., Davoodi, M., Jafari, M.K., (2013). Correlation between settlement of embankment dams and ground motion intensity indices of pulse-like records. Iranian Journal of Science and Technology Transactions of Civil Engineering 37 (1), 111–126.

11. Zhang, S., Wang, G., Pang, B., Du, C. (2013). The effects of strong motion duration on the dynamic response and accumulated damage of concrete gravity dams. Soil Dyn Earthq Eng 45:112–124.
12. Akköse, M., Şimşek, E. (2010). Non-linear seismic response of concrete gravity dams to near-fault ground motions including dam-water-sediment-foundation interaction. Appl Math Model 34(11):3685–3700.
13. Chopra, A.K., Chintanapakdee, C., (2001a). Comparing response of SDF systems to near-fault and far-fault earthquake motions in the context of spectral regions. Earthquake Engineering and Structural Dynamics 30, 1769–1789.
14. Davoodi, M., Jafari, M.K., and Hadiani, N. (2013). Seismic response of embankment dams under near-fault and far-field ground motion excitation. Engineering Geology, Vol. 158, pp. 66–76.
15. Bayraktar, A., Altunıs, ık A.C., Sevim, B., Kartal, M.E., Turker, T. (2008). Near-fault ground motion effects on the non-linear response of dam-reservoir-foundation systems. Struct Eng Mech 28(4):411–442.
16. Wang, G., Zhang, S., Wang, C., Yu M. (2014). Seismic performance evaluation of dam-reservoir-foundation systems to near-fault ground motions. Nat Hazards 72, 651–674.
17. Yazdani, Y., and Alembagheri, M. (2017). Non-linear seismic response of a gravity dam under near-fault ground motions and equivalent pulses. Soil Dynamics and Earthquake Engineering, Vol. 92, pp. 621–632.
18. Ghanaat, Y. (2002). Seismic performance and damage criteria for concrete dams. In: Proceedings of the 3rd US-Japan workshop on advanced research on earthquake engineering for dams, San Diego p. 22–23.
19. Ghanaat, Y. (2004). Failure modes approach to safety evaluation of dams. In: 13th World conference on earthquake engineering, Vancouver, Paper no. 1115.
20. Liao WI, Loh CH, Lee BH. (2004). "Comparison of dynamic response of isolated and nonisolated continuous girder bridges subjected to near-fault ground motions." Engineering Structures, 26(14):2173–83.
21. Chen, G.L., Lu, W.Z., Wang, L., Wu, Q., (2013). Study on Far-Field Ground Motion Characteristics. Applied Mechanics and Materials 438–439, 1471–1473. 438-439.1471.
22. Dicleli, M., and Buddaram, S. (2007). Equivalent linear analysis of seismic-isolated bridges subjected to near-fault ground motions with forward rupture directivity effect. Engineering Structures, 29(1):21–32.
23. ASCE. (2016). Minimum Design Loads and Associated Criteria for Buildings and Other Structures. ASCE/SEI 7, Reston, Virginia.
24. BIS (Bureau of Indian Standards). (1984). Criteria for earthquake resistant design of structures. IS 1893, New Delhi, India.
25. BIS (Bureau of Indian Standards). (2000). Plain and reinforced concrete-code of practice. IS 456, New Delhi, India
26. BIS (Bureau of Indian Standards). (2013). Criteria for design of solid gravity dams. IS 6512, New Delhi, India.

27. Raphel, J.M. (1984). Tensile strength of concrete. ACI J Proc 81(2):158–165.
28. https://ngawest2.berkeley.edu/
29. BIS (Bureau of Indian Standards). (2016). Criteria of Earthquake Resistant Design of Structures: General Provisions and Buildings. IS 1893-Part 1, New Delhi, India.
30. Mollaioli, F., Bruno, S., Decanini, L.D. et al. (2006), Characterization of the Dynamic Response of Structures to Damaging Pulse-type Near-fault Ground Motions. Meccanica 41, 23–46.